Detection and Quantification of *Leveillula taurica* Growth in Pepper Leaves

Zheng Zheng, Teruo Nonomura, Károly Bóka, Yoshinori Matsuda, Richard G. F. Visser, Hideyoshi Toyoda, Levente Kiss, and Yuling Bai

First, fifth, and eighth authors: Wageningen UR Plant Breeding, Wageningen University & Research Center, Droevendaalsesteeg 1, 6708PB Wageningen, The Netherlands; second, fourth, and sixth authors: Laboratory of Phytoprotection Science and Technology, Faculty of Agriculture, Kinki University, Nara 631-8505, Japan; third author: Department of Plant Anatomy, Eötvös Loránd University, H-1117 Budapest, Pázmány Péter sétány 1/C, Hungary; and seventh author: Plant Protection Institute, Centre for Agricultural Research, Hungarian Academy of Sciences, H-1525 Budapest, P.O. Box 102, Hungary.

Accepted for publication 9 January 2013.

ABSTRACT

Zheng, Z., Nonomura, T., Bóka, K., Matsuda, Y., Visser, R. G. F., Toyoda, H., Kiss, L., and Bai, Y. 2013. Detection and quantification of *Leveillula taurica* growth in pepper leaves. Phytopathology 103:623-632.

Leveillula taurica is an obligate fungal pathogen that causes powdery mildew disease on a broad range of plants, including important crops such as pepper, tomato, eggplant, onion, cotton, and so on. The early stage of this disease is difficult to diagnose and the disease can easily spread unobserved; for example, in pepper and tomato production fields and greenhouses. The objective of this study was to develop a detection and quantification method of *L. taurica* biomass in pepper leaves with special regard to the early stages of infection. We monitored the development of the disease to time the infection process on the leaf surface as well as inside the pepper leaves. The initial and final steps of the infection taking place on the leaf surface were consecutively observed using a dissecting microscope and a scanning electron microscope. The development of the intercellular mycelium in the mesophyll was followed by light and transmission electron microscopy. A pair of *L. taurica*-specific primers was designed based on the internal transcribed spacer sequence of *L. taurica* and used in real-time polymerase chain reaction (PCR) assay to quantify the fungal DNA during infection. The specificity of this assay was confirmed by testing the primer pair with DNA from host plants and also from another powdery mildew species, *Oidium neolycopersici*, infecting tomato. A standard curve was obtained for absolute quantification of *L. taurica* biomass. In addition, we tested a relative quantification method by using a plant gene as reference and the obtained results were compared with the visual disease index scoring. The real-time PCR assay for *L. taurica* provides a valuable tool for detection and quantification of this pathogen in breeding activities as well in plant–microbe interaction studies.

Powdery mildew is a serious fungal threat to agricultural production. The endoparasitic powdery mildew fungus *Leveillula taurica* (Lév.) G. Arnaud (anamorph: *Oidiopsis taurica* (Lév.) E. S. Salmon) is an important pathogen of pepper, tomato, eggplant, onion, cotton, and other crops, and it has also been recorded on many wild plant species (4). This pathogen represents a challenge from many perspectives. First, the early stages of infection are difficult to diagnose; thus, the disease can rapidly spread in both field and greenhouse crop production. Second, the species delimitation in the genus *Leveillula* is problematic and the binomial "*L. taurica*" clearly refers to a species complex that includes several biological species (13–15). Moreover, the exact host ranges of the different *L. taurica* lineages recognized by phylogenetic studies are still not known (14).

Most powdery mildew species are epiparasitic because all their structures except haustoria are developed on the host plant surfaces. In contrast, *Leveillula* and the other genera in tribe *Phyllactinieae,* namely *Phyllactinia* and *Pleochaeta*, develop a partly endophytic mycelium and are endotrophic because their haustoria are produced in the mesophyll cells. Kunoh et al. (17) illustrated that, in *L. taurica*, the germinated conidia are attached to the leaf surface by "adhesion bodies" that differ from appressoria produced by epiphytic species because they do not initiate infection hyphae that penetrate the epidermal cells. Instead, infection hyphae of *L. taurica* enter the host plant through stomata and develop an intercellular mycelium in the spongy and palisade parenchyma tissue with haustoria in some of its cells. Later, conidiophores emerge through stomata, mainly on the abaxial leaf surface, producing primary and numerous secondary conidia that differ in their morphology (4). At that stage, hyphae are also produced mainly on the abaxial leaf surfaces. On the adaxial surface of infected leaves, chlorotic spots are usually visible, indicating the development of mildew colonies underneath the spots.

For studies on plant–microbe interactions and in practical breeding programs for disease resistance, detection, monitoring, and quantification of the pathogen are crucial steps. Depending on the characteristics of the pathogen, there are numerous methods to quantify the amount of pathogen present in the host plants. Such methods include visual inspection, digital image analysis, histological analysis, light microscopic methods, immunological techniques, biochemical quantification of microorganism compounds, and nucleic acid-based technologies (2,3,18,33). The simplest way to evaluate the level of disease in plants is based on the visual evaluation of symptoms using disease index (DI) values. This method is fast, easy, and normally does not require any extra equipment. However, the visual inspection has drawbacks. First, the disease symptoms have to be visible on the plant

Corresponding author: Y. Bai, E-mail address: bai.yuling@wur.nl

*The *e*-Xtra logo stands for "electronic extra" and indicates that the online version contains three supplemental figures and one supplemental video.

http://dx.doi.org/10.1094/PHYTO-08-12-0198-R

tissues. Second, the evaluation is subjective. Third, it is hard to distinguish the small differences between intermediates. To overcome the drawbacks, other methods, such as enzyme-linked immunosorbent assay and measurements of pathogen specific components such as chitin and ergosterol, have been developed (10,11,23,25). However, the use of these methods in daily research and breeding activities is also limited by factors such as the specificity of detection probes, laborious process, and expensive materials. Another technique, real-time polymerase chain reaction (PCR) assay, can quantify PCR amplicons by measuring the fluorescent signals. Due to its rapidity, sensitivity, reproducibility, and high specificity, it has quickly become a popular method for pathogen detection and quantification (35).

Thus far, the disease scoring system for *L. taurica* is mainly based on visual inspection of leaves. By scoring symptoms, Shifriss et al. (29) included the infected plants in three groups: symptomless, susceptible, and intermediate. Others such as Souza et al. (7) counted the latency period: days from inoculation till the appearance of *L. taurica* conidia on plants. To date, the most accurate disease scoring method for *L. taurica* is the synthetic DI described by Daubèze et al. (6), which has been used for a quantitative trait loci mapping study (19). This synthetic DI sums up two parameters in order to represent a good indication of resistance. One parameter is the disease symptom represented by the proportion of infected leaves per plant with a scale from 0 to 5 (0 = no infected leaves to 5 = the whole foliage infected). The other one is the sporulation intensity with, again, a 0-to-5 scale (6,19). However, the main difficulty of all these scoring methods is how to evaluate the size or the density of individual mildew colonies.

The main goals of the present work were to follow the infection process of *L. taurica* in pepper leaves and to develop an objective scoring methodology. We attempted to monitor the development of the pathogen to time the infection process by using different microscopic techniques, such as a high-fidelity digital microscope and scanning electron microscopy (SEM) for the study of the infection steps on the leaf surface, and light and transmission electron microscopy (TEM) for steps taking place inside the leaves. To quantify the pathogen biomass, we developed a real-time PCR assay and measured the *L. taurica* DNA amount (absolute and relative to plant DNA) in infected plant tissues.

MATERIALS AND METHODS

Disease assay. To develop a disease scoring system, and also for the real-time PCR studies, the powdery mildew pathogen *L. taurica* was collected from infected pepper plants in a greenhouse in The Netherlands and maintained on pepper plants of a susceptible cultivar ('Maor'). The inoculation was performed on 6-week-old plants. Conidia of *L. taurica* were washed off with water from heavily infected pepper leaves. Inoculum was adjusted to a final concentration of 2.5×10^4 conidia/ml, and sprayed onto the abaxial surface of the leaves. Inoculated plants were kept for 24 h in plastic cages in the greenhouse with 100% relative humidity at 21°C. Then, the temperature and humidity were adjusted to 21°C (day) and 19°C (night) and relative humidity 70% in the greenhouse.

To perform light microscopy and TEM studies, the pathogen was maintained on potted pepper 'Cibere F1' plants in an experimental greenhouse in Hungary. The environmental factors and the inoculation method were similar to those applied in the Dutch greenhouse.

To carry out the digital microscopic analysis, pepper (*Capsicum annum* L. 'Kyounami') was used in this study in Japan. Seed were placed on wet filter papers in petri dishes and germinated for 3 to 4 days in a growth chamber under continuous illumination (4,000 lux) at 25 ± 2°C. Then, 14-day-old seedlings (one to two folded leaves) were used for inoculation with *L. taurica* conidia. For maintaining the pathogen, inoculum was made and sprayed onto leaves of 14-day-old seedlings of pepper according to the method of Bai et al. (1). Inoculated seedlings were placed for 1 month in a growth chamber with 70 to 80% relative humidity at 20 ± 1°C under continuous illumination of 4,000 lux. Newly produced conidia were used as inoculum for next-round inoculation to maintain the pathogen as described earlier.

Macroscopic disease scoring. We modified the disease scoring method of Daubèze et al. (6) based on the scoring method described by Bai et al. (1) for *O. neolycopersici*. DI was used to score the sporulation intensity of *L. taurica* on each infected leaf. This DI system was based on a scale of 0 to 5, where 0 = no visible sporulation, 1 = restricted chlorotic spots on the adaxial leaf surface, with weak or no sporulation on the corresponding abaxial leaf areas; 2 = several isolated sporulation spots on the abaxial leaf area; 3 = numerous sporulation spots covering up to 40 to 50% of the abaxial leaf area; 4 = numerous coalescent sporulation spots covering up to 75% of the abaxial leaf area; and 5 = the whole abaxial surface of the leaf, and also parts of the adaxial leaf surface, covered with dense sporulation. The third, fourth, and fifth true leaves were scored for each plant.

Light microscopy. To study the epiphytic fungal structures on the abaxial leaf surfaces as well as the penetration process through stomata and the production of haustoria in the mesophyll cells, samples were prepared in the following ways for light microscopy. (i) Leaf segments of approximately 1 by 3 cm in size were collected from powdery mildew-infected pepper plants in a greenhouse and fixed in acetic acid/ethanol (1:3), followed by staining with 0.03% trypan blue in lactophenol/ethanol (1:3), as described by Bai et al. (1). (ii) Mature conidia of *L. taurica* were collected from conidiophores formed on pepper leaves using an electrostatic spore collection probe described previously (24) and transferred onto leaves of 1-month-old seedlings of pepper for inoculation. Inoculated seedlings were incubated in a growth chamber with 70 to 80% relative humidity at 20 ± 1°C under continuous illumination of 4,000 lux. Leaf segments collected in the same way were decolorized in a boiling alcoholic lactophenol solution for 1 to 2 min, and stained with aniline blue, according to Sameshima et al. (26). More than 100 samples were used for observation of infection steps of *L. taurica* on the surface of pepper leaves. (iii) Leaves collected from powdery mildew-free Cibere F1 pepper plants, grown in isolation in a climate chamber, were placed with their abaxial surfaces up in glass petri dishes of 9 cm in diameter, on polystyrene balls floated on sterile water. The abaxial leaf surfaces were inoculated by dusting *L. taurica* conidia onto their surfaces; then, the plates were closed and kept at 25°C at continuous light for 48, 72, and 96 h. At each time interval, small pieces were cut out of the inoculated leaves where germinated conidia were observed under a dissecting microscope, macerated in a droplet of water or boiled in lactic acid on a microscope slide, occasionally stained with cotton blue in lactophenol, and examined under a light microscope.

Digital microscopy. Conidia were collected from conidiophores developed on infected leaves and transferred to the abaxial leaf surfaces (one conidium per leaf), using a glass needle installed with micromanipulator and a high-fidelity digital microscope (KH-2700; Hirox, Tokyo) (24). To show the conidial germination and the penetration process in an animated way, the conidia were photographed on the abaxial surface of a pepper leaf at 0.5- to 1-h intervals for 48 h after inoculation using a CCD-camera of the digital microscope. Photographs were treated using an image processing software (Adobe Photoshop, ver. 5; Adobe Systems, San Jose, CA), and 110 image-analyzed photographic data were input to a Windows live movie maker software (Microsoft, Redmond, WA). The photographic data collected at 3 to 4 and 18 to 30 h after inoculation were analyzed for conidial germination and penetration. This experiment was carried out five times.

SEM. Pepper leaves infected with *L. taurica* were fixed in 0.1 M phosphate buffer (0.1 M NaH_2PO_4 and 0.1 M Na_2HPO_4) containing 2.5% glutaraldehyde at pH 7.4 for 1 day, and postfixed in 1% osmium tetroxide (Nacalai tesque, Kyoto, Japan) in the same buffer for 2 h. The fixed leaves were dehydrated through graded ethanol series (50 to 99.8%) and then soaked in t-butyl alcohol (Nacalai tesque) for 20 min at room temperature. The samples were frozen at 4°C for 2 h and dried using a freeze-drying device (JFD-300; JEOL Ltd., Tokyo). The dried leaves were coated with platinum-palladium metal particles using an ion sputtering device (JFD-1100E; JEOL Ltd.) and observed with a scanning electron microscope (JSM-6510LA; (JEOL Ltd.).

TEM. Pepper leaf segments infected with *L. taurica*, ≈5 by 5 mm in size, were fixed in 2% glutaraldehyde for 3 h and in 1% osmium tetroxide for 2 h (both fixatives were dissolved in 0.1 M K-Na-phosphate buffer at pH 7.2) and embedded in Durcupan resin after dehydration in an ethanol series ended with propylene oxide. Two to four leaves were sampled for each of the five DI values determined, as described above. Semithin sections (1 µm) for light microscopy were prepared with a Microm HM 360 microtome (Microm, Walldorf, Germany) and stained with toluidine blue. Ultra-thin sections (70 nm) were cut with a Reichert Ultracut E ultramicrotome (Leica Microsystems, Vienna, Austria) mounted on uncoated Cu/Pd grids (Polysciences, Warrington, PA), and stained with 5% uranyl acetate dissolved in methanol for 4 min and lead citrate for 6 min. Sections were viewed with a Hitachi 7100 transmission electron microscope (Hitachi, Tokyo) at an accelerating voltage of 75 kV and a JEOL JEM 1011 transmission electron microscope (JEOL Ltd.) at 60 kV.

Primers used for real-time PCR. Internal transcribed spacer (ITS) sequences of *L. taurica* infecting pepper were retrieved from GenBank and specific primers were designed by using the online software Primer3 plus (http://www.bioinformatics.nl/cgi-bin/primer3plus/primer3plus.cgi). The forward primer LV-F (5′AGCCGACTAGGCTTGGTCTT3′) and the reverse primer LV-R (5′GCGGGTATCCCTACCTGATT3′) amplified a 208-bp fragment. The housekeeping gene *CaActin*, as a plant reference gene, was amplified from pepper leaves using the forward primer CaActin-F (5′ATCCCTCCACCTCTTCACTCTC3′) and the reverse primer CaActin-R (5′GCCTTAACCATTCCTGTTCCATTATC3′), as described by Silvar et al. (30).

DNA isolation. *L. taurica* conidia (Fig. 1, lower panel), as free of any contamination as possible, were collected in a glass vial with a vacuum pump-operated cyclone spore collector (34) from heavily infected pepper plants in the greenhouse of Wageningen University. Conidia were disrupted by grinding them in liquid nitrogen. DNA was isolated using the DNeasy Kit including the RNAse treatment (Qiagen, Hilden, Germany). Two independent DNA samples were isolated for biological replicates.

Powdery-mildew-infected pepper leaves which were assigned to different DI classes by visual inspection scoring were collected and ground in liquid nitrogen. Three plants per DI class were used. Two infected leaves per plant were pooled for sampling and three pools were made for each plant. DNA was isolated using the DNeasy Kit (Qiagen) and DNA quality was checked by NanoDrop ND-1000, UV-Vis spectrophotometer (NanoDrop Technologies, Wilmington, DE). The concentration of each sample was adjusted to 15 ng/µl.

Real-time PCR. Real-time PCR was performed by using the SYBR Green dye on Bio-Rad iCycleriQ machine. PCR reactions were made by mixing 5 µl of iQ SYBR Green Supermix (Bio-Rad Hercules, CA) with 0.3 µl of each primer (10 µM) and 1 µl of DNA template (15 ng/µl). Each PCR reaction was done in triplicate in a total volume of 10 µl. PCR reactions were done with the following program: 1 cycle at 95°C (3 min), 40 cycles of denaturation at 95°C (15 s) and primer annealing and extension at 60°C (60 s), and 1 cycle at 95°C (60 s). Finally, melting curve analysis was performed from 65 to 95°C (0.5°C per cycle of 61 s). The pepper gene *CaActin* was used as a reference to normalize the DNA proportion of plant by ΔΔ threshold cycle (Ct) methods (20).

RESULTS

Infection steps of *L. taurica* on pepper leaf surfaces. Conidia germinated and formed primary adhesion bodies at the ends of the first germ tubes 3 to 4 h following inoculation of the abaxial pepper leaf surfaces (Fig. 2A; Supplemental Video). From primary adhesion bodies, infection hyphae emerged which either quickly penetrated the leaf tissues through stomata starting from 6 h (Fig. 2B) or continued to grow on the leaf surface, sometimes even through the nearest stoma, branched (Fig. 2C), and produced secondary (or hyphal) adhesion bodies (Fig. 2D) before penetrating the leaf through a stoma. The primary and the hyphal adhesion bodies were clearly distinguished from each other based on their distinct shapes. Those hyphae that did not branch on the leaf surface following their emergence from primary adhesion bodies entered the leaf tissues through stomata within 24 h following inoculation, while the tips of the branched hyphae entered stomata at different time intervals; for example from 30 to

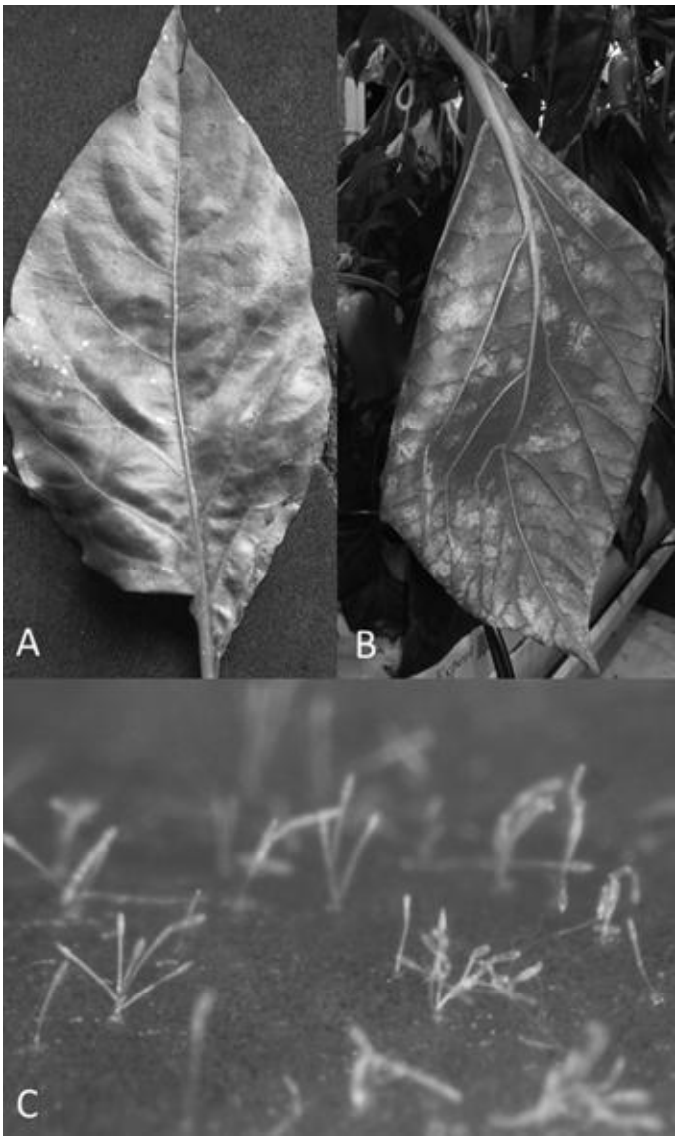

Fig. 1. A, Disease symptom (lighter spots) on adaxial leaf surface and **B,** white fungal colonies on abaxial leaf surface of a susceptible pepper cultivar in a production greenhouse. **C,** Mature *Leveillula taurica* conidiophores emerging from stomata on the abaxial leaf surface.

48 h after inoculation. The pathogen projected hyphae and conidiophores from stomata 14 to 16 days after inoculation (Fig. 2E). The hyphae vigorously elongated and formed many secondary adhesion bodies on the leaf surface (Fig. 2F). Mature conidia produced on conidiophores became the sources of subsequent infections (Fig. 1).

Infection steps inside pepper leaves. The pathogen did not produce haustoria in epidermal cells because neither semithin sections observed using light microscopy (Fig. 3) nor the TEM study revealed haustoria in the epidermis. The absence of penetration pegs underneath 26 primary and 36 secondary adhesion bodies examined in this study has also suggested the lack of haustoria in those cells (Fig. 4).

After entering the leaf tissues through stomata, the powdery mildew hyphae continued their growth intercellularly in the spongy parenchyma tissue, without swelling in the substomatal cavities which is known for infection by rust fungi (Figs. 3 and 5A). Intercellular hyphae were detected even in the veins, among the cells of the vascular tissues (Fig. 5B). The septal pores with Woronin bodies attached to the septa with thin filamentous structures were also observed in the intercellular hyphae (Supplemental Figure 1). Mesophyll cells were entered by penetration pegs arising from intercellular hyphae (Fig. 5C). These were always surrounded by papillae consisting of thinner electron-dense and much thicker electron-lucent, callose-like materials (Fig. 5C and D; Supplemental Figure 2). Penetration pegs continued their intracellular development and gave rise to haustoria. In none of the observed plant cells did papillae arrest the development of haustoria. The fully developed haustorium consisted of a central body and several lobes embedded in a haustorial matrix (Fig. 6A) and surrounded by an extrahaustorial membrane (Fig. 6B). Large spherical structures, up to 1 to 1.2 μm diameter, resembling lipid bodies, were seen inside the central bodies and lobes of haustoria, in the haustorial matrices, and also outside the extrahaustorial membrane, in the cytoplasm of the invaded parenchyma cells (Fig. 6C). Such voluminous structures did not appear in the uninfected plant cells. Chloroplast architecture was also altered in the infected parenchyma cells: the grana were

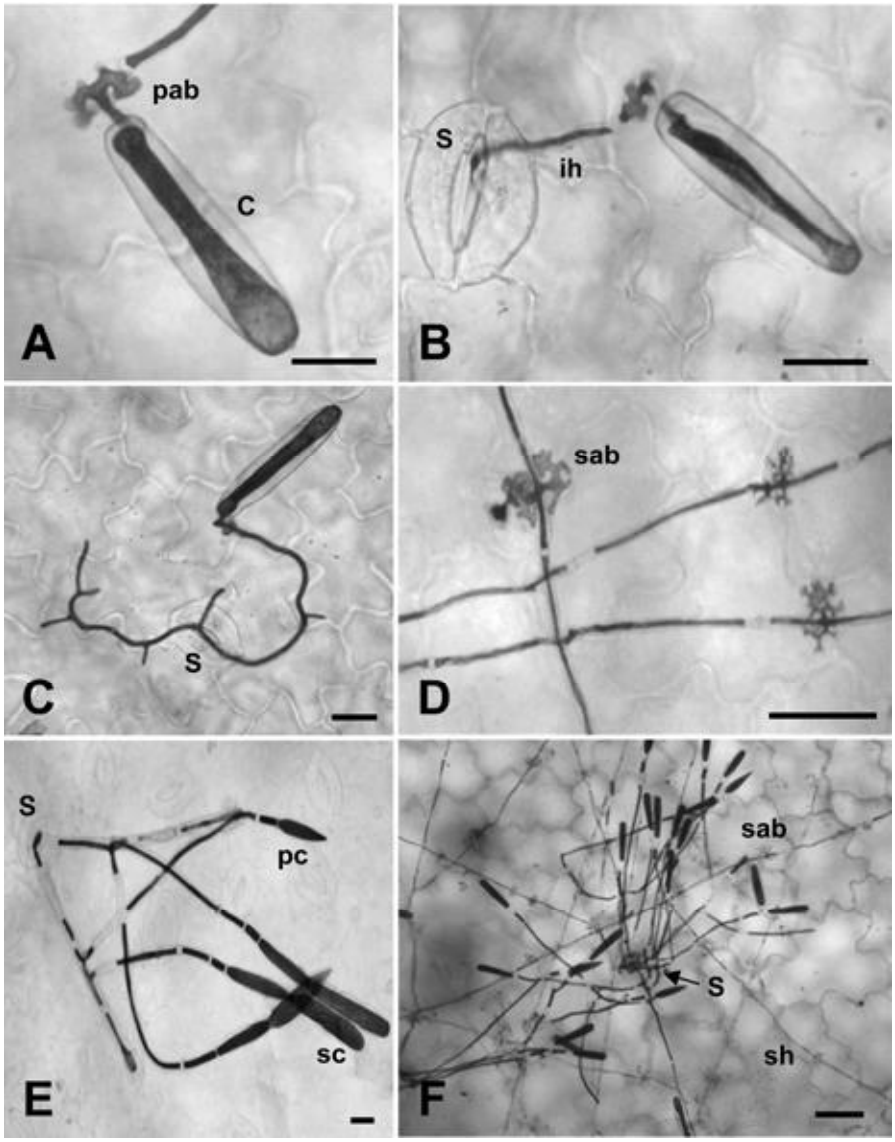

Fig. 2. Infection steps of *Leveillula taurica* on the abaxial surface of pepper leaves. **A,** Germinated conidia (c) produce lobed primary adhesion bodies (pab). **B,** These initiate infection hyphae (ih) that penetrate the leaves through stomata (s). **C,** Before entering the nearest stoma (s), these hyphae sometimes continue their growth epiphytically and branch on the abaxial leaf surfaces. **D,** Branched superficial hyphae produce secondary adhesion bodies (sab). **E,** Conidiophores start to emerge from stomata (s) approximately 14 to 20 days following inoculation. Primary conidia (pc) produced on conidiophores are lanceolate whereas secondary conidia (sc) are ellipsoid to cylindrical. **F,** Superficial hyphae (sh) appear from conidiophores emerged from stomata (s), continue their growth epiphytically, attach to the leaf surfaces with secondary adhesion bodies (sab), and produce new conidiophores with primary and secondary conidia. Bars = 20 μm (A to E) and 100 μm (F).

organized in larger structures and the chloroplasts contained large plastoglobuli, ≤0.8 to 1 μm diameter (Fig. 6D; Supplemental Figure 3). The nucleus of some of the infected plant cells exhibited a lobed shape (Fig. 6D). Both the altered chloroplast structure and the lobed nucleus shape are characteristic of plant cells exposed to various stress factors (27). The first haustoria were observed in the mesophyll cells of leaf macerates 72 to 96 h following inoculations. At this stage, the infected leaves were completely symptomless, although the pathogen had already been established in the mesophyll.

DNA standard curve for *L. taurica*. The LV-F/LV-R primer pair developed in this work amplified a specific fragment of the ITS region of *L. taurica*. To verify the specificity of these primers, DNA was isolated from *O. neolycopersici* conidia as well as from powdery-mildew-free pepper leaves. These two DNA samples were used as templates in a real-time PCR with LV-F and LV-R primers. No amplicons were detected from plant DNA samples on agarose gel after 40 cycles of amplification and, furthermore, the melting curve analysis of the PCR products did not retrieve any unexpected amplicons. Thus, the developed LV-F/LV-R primer pair was suitable for the diagnosis and quantification of *L. taurica* from pepper leaves.

In a real-time PCR plotting assay, a standard curve could be constructed to express the equivalent relation between the cycle numbers and the concentration of a given substance in the template. For pathogen quantification, a standard curve is normally generated by plotting the cycle numbers of a pathogen DNA dilution series against the known concentration of the pathogen. In this study, a standard curve for *L. taurica* was generated by amplifying a dilution series of *L. taurica* genomic DNA. Starting from 5,800 pg of DNA, dilutions were done in six steps with 10-fold dilution per step. A standard curve was obtained by plotting the Ct (in the Y axis) against the genomic DNA concentration of *L. taurica* (in the X axis) (Fig. 7). A linear correlation ($R^2 = 0.9978$) was obtained between the Ct values and the *L. taurica* DNA concentration. The melting curve analysis of the PCR samples retrieved only a single peak. Additionally, a primer pair specific for the pepper housekeeping gene *CaActin* was used to check whether the *L. taurica* DNA is free of pepper DNA contamination. With the *L. taurica* DNA samples, no PCR products were detected after 40 cycles of amplification using the primer pair for *CaActin*. Thus, there was no pepper DNA contamination in the collected *L. taurica* DNA samples used in this study. The experiments were repeated with different sets of samples and the obtained standard curves supported the stability of this assay.

Detection and quantification of *L. taurica* mycelium in pepper plants. Although the absolute amount of the pathogen in the host tissues was determined by using the DNA standard curve of *L. taurica* mycelium, results were not normalized with the amount of plant tissues used during the isolation of fungal DNA. Therefore, it was necessary to quantify the relative amount of pathogen DNA in infected plant tissues by measuring both fungal and plant DNA in the same samples. To do so, we used plant gene *CaActin* as reference to normalize the *L. taurica* DNA concentration in the infected sample. Five pepper cultivars were selected which showed different levels of susceptibility against *L. taurica* in the greenhouse. First, the DI values were determined for each cultivar. As a second step, DNA was isolated from *L. taurica*-infected leaves. Two real-time PCR reactions were performed with the same DNA sample by using primers specific to plant and fungal DNA. The quantities of *L. taurica* DNA in different samples were normalized by plant DNA using ΔΔCt methods (20) (Fig. 8). A good correlation was obtained between real-time PCR and the DI values; pepper plants displaying mild mildew symp-

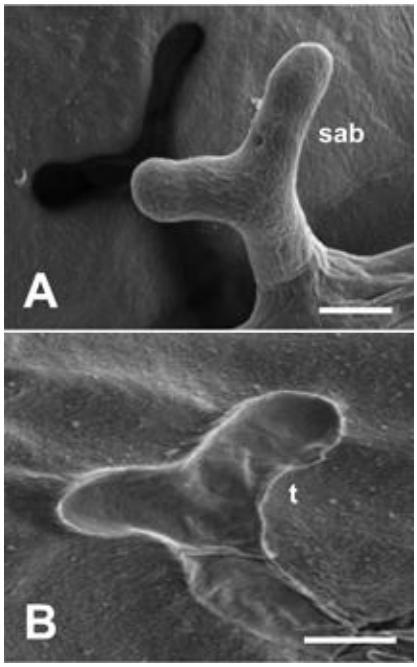

Fig. 4. Scanning electron micrographs showing the tracks of secondary adhesion bodies produced on superficial hyphae of *Leveillula taurica* on abaxial surfaces of pepper leaves. **A,** Secondary adhesion body (sab) lifted up from the leaf epidermis by micromanipulation. **B,** Track (t) of a secondary adhesion body developed 48 h after inoculation and removed by micromanipulation. Note the absence of any penetration hole in the track. Bars = 2 μm.

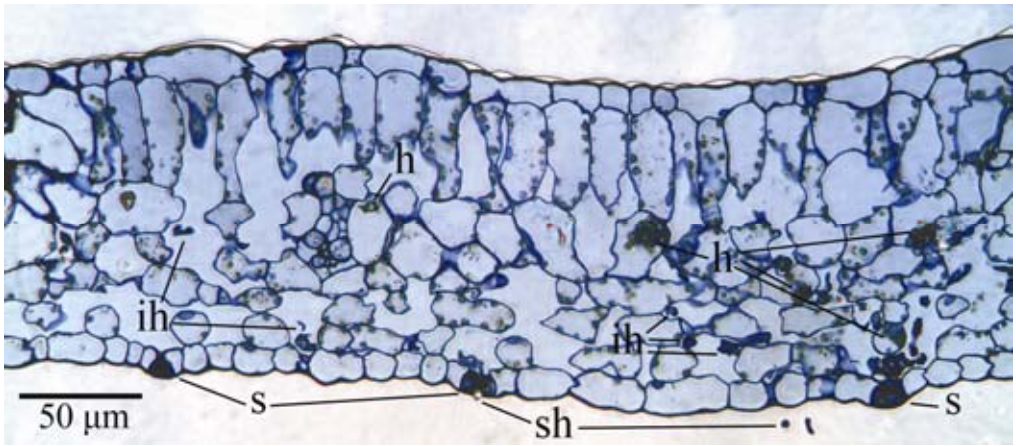

Fig. 3. Semithin section of a pepper leaf infected with *Leveillula taurica* and stained with toluidine blue. Intercellular hyphae (ih) and haustoria (h) are present in the cells of the spongy parenchyma tissue. Superficial hyphae (sh) are also seen on the adaxial leaf surface, sometimes in close vicinity of stomata (s).

toms contained a lower fungal DNA amount and vice versa (Fig. 8). This relative quantification method is useful to distinguish small differences in mycelial biomass that is proportional with disease severity.

DISCUSSION

Thus far, only a few histological studies have been carried out to follow some steps of the infection process of *L. taurica*. These earlier studies focused on the morphological characteristics of the pathogen on pepper leaf surfaces such as the morphology of its germ tubes (5,12), primary adhesion bodies (12,17), secondary adhesion bodies (12), and conidiophores (32). However, none of these works timed or quantified the development of the *L. taurica* mycelium on the surface and inside the infected pepper leaves. The present work is the first comprehensive survey that achieved this goal based on structural, ultrastructural, and molecular studies. We first followed the infection process starting from conidial germination on the abaxial leaf surface. A consecutive observation of this process under a stereomicroscope led to a full description of the first steps of the infection. Light microscopy and a TEM study of the infected leaf tissues confirmed the earlier findings regarding the lack of *L. taurica* haustoria in the epidermal cells, the sole targets of the haustoria of those powdery mildew species which, in contrast to *L. taurica*, produce hyphae only on the surfaces of their host plants. In fact, *L. taurica* also develops haustoria in a sole cell type only; namely, the cells of the spongy and palisade parenchyma. These were detected as early as 3 to 4 days postinoculations. Our results supported the TEM work by Kunoh et al. (17) and, in addition, we have shown that conidial germination is followed by the development of branched hyphae on the abaxial leaf surfaces, in addition to the production of primary (infection) hyphae which quickly enter the leaves through stomata. We have also distinguished primary and secondary adhesion bodies on these epiphytic hyphae and have shown the presence of *L. taurica* intercellular hyphae in the vascular tissues of the leaves. Recently, Micali et al. (22) demonstrated that papillae produced in the epidermal cells of *Arabidopsis thaliana* infected with the epiphytic powdery mildew species *Golovinomyces orontii* contain callose (β-1,3-glucan). Because the papillae examined in this work (Fig. 5C and D) were morphologically similar to those seen in the *Arabidopsis–Golovinomyces* interaction, we supposed that the electron-lucent materials observed around the penetration pegs are made of callose, as well. Also, similar to the *Arabidopsis–Golovinomyces* interaction, membranous and vesicular structures were observed in the callose

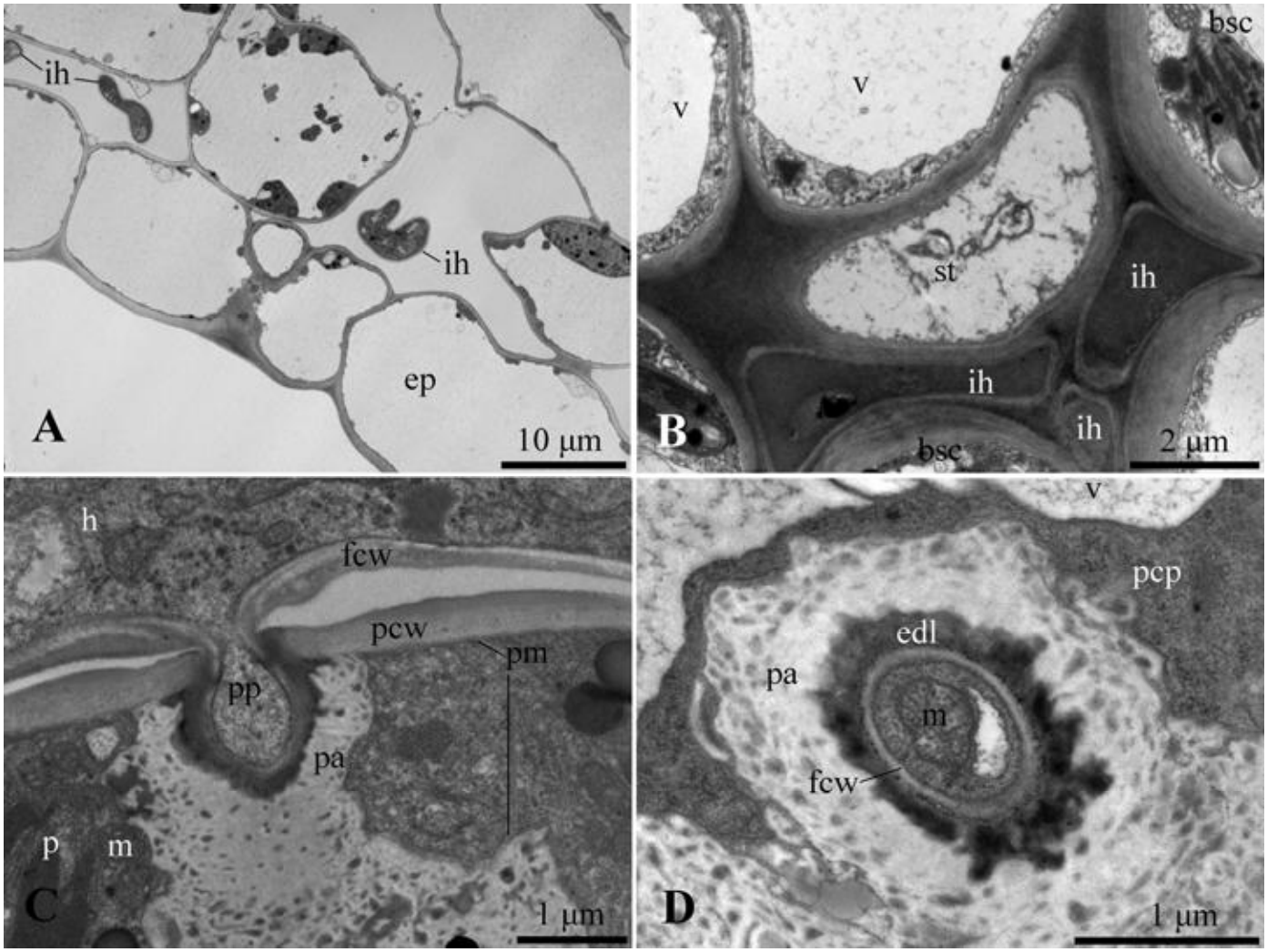

Fig. 5. Transmission electron micrographs of *Leveillula taurica* hyphae inside pepper leaves. **A,** Early stage of infection with intercellular hyphae (ih) in a substomatal cavity and also in the regular intercellular spaces below the epidermis (ep). **B,** Intercellular hyphae (ih) in a leaf vein and among sieve tube (st) and vascular bundle sheath cells (bsc); v = vacuole. **C,** Almost longitudinal section through a penetration peg (pp) emerged from an intercellular hypha (h) in the mesophyll and surrounded by a papilla (pa); fcw = fungal cell wall; m = mitochondrion; p = plastid; pcw = plant cell wall; pm = plasma membrane. See also Supplemental Figure 2 for more details. **D,** Transversal section through a penetration peg surrounded by a papilla (pa) consisting of an electron-dense layer (edl) around the fungal cell wall (fcw) and an electron-lucent layer; pcp = plant cytoplasm; m = mitochondrion; v = vacuole.

layer surrounding penetration pegs. Callose encasement of haustoria was observed, as well (Fig. 6C), but it was not as prominent as in the case of *Arabidopsis* epidermal cells invaded by *G. orontii* haustoria (22).

The TEM study has also revealed structural changes in the organelles of pepper cells containing *L. taurica* haustoria. The multilobed nucleus (Fig. 6D) and the presence of enlarged and flattened grana in the chloroplasts of the infected cells have already been described as the results of various biotrophic plant–microbe interactions (8,27).

This study showed that the latency period of the *L. taurica* infection may last for >2 weeks following conidial germination on the abaxial leaf surfaces. A comprehensive work on pepper powdery mildew has revealed that this period is different in various pepper cultivars and, in addition, it strongly depends on the age of the infected pepper plants, being shorter in older plant tissues (7). Due to the long latency period of the *L. taurica* infection, the early diagnosis of the pathogen is almost impossible before mildew colonies become visible as white patches. Even with symptoms, it is also difficult to evaluate the disease severity in practice, such as during resistance breeding programs. In this study, we developed two real-time PCR assays for quantification of *L. taurica* mycelium using ITS sequences. These sequences were recently proposed as official DNA barcodes for the fungal kingdom (28) in spite of some limitations (16). At present, real-time PCR identification, detection, and quantification of pathogens is widely used in medical diagnosis, plant–microbe interaction studies, and breeding programs (3,21). With the standard curve (Fig. 7) developed in this study, absolute quantification of the pathogen DNA can be obtained. On the other hand, the relative quantification method developed in this work allows the measurement of the ratio between fungal DNA and host plant DNA in the same sample (Fig. 8), similar to other works (9,37). By testing a set of *L. taurica*-infected pepper plants showing different levels of resistance, the correlation between the DI values and amount of fungal DNA confirmed the sensitivity and robustness of the relative quantification method (Fig. 8). The fact that no amplicon could be detected in the reactions when using DNA of uninfected plants and other powdery mildews demonstrates the specificity of both assays.

In most cases, genomic DNA was used as template in the PCR assay. There is evidence that the DNA content could vary in different pathogen organs. Therefore, several studies had been carried out to use RNA as template in the PCR assay (36). How-

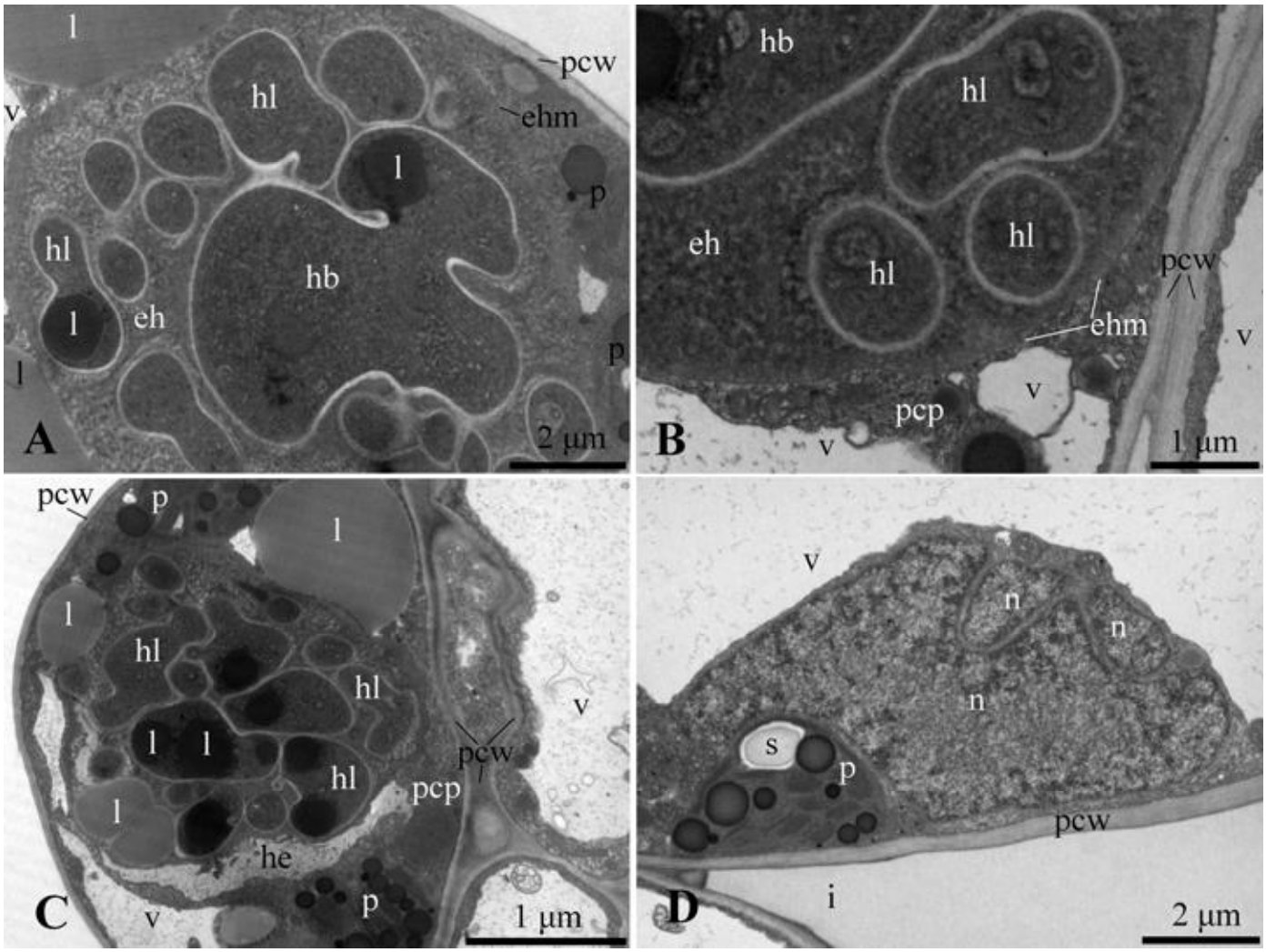

Fig. 6. Transmission electron micrographs showing haustoria of *Leveillula taurica* and the ultrastructure of the infected mesophyll cells. **A,** Haustorium consisting of a haustorial body (hb) and several haustorial lobes (hl) embedded in an extrahaustorial matrix (eh) and surrounded by an extrahaustorial membrane (ehm). Note lipid bodies (l) inside the haustorium and also in the plant cytoplasm; p = plastid; pcw = plant cell wall; v = vacuole. **B,** Details of a haustorium developed close to the plant cell wall (pcw). Note the structural differences between the extrahaustorial matrix (eh) and the plant cytoplasm (pcp); hb = haustorial body; hl = haustorial lobe; ehm = extrahaustorial membrane; v = vacuole. **C,** Lipid deposition inside and outside a haustorium in an infected pepper cell. Lipid bodies (l) are present in the plant cytoplasm (pcp) as well as in the haustorial lobes (hl) and the extrahaustorial matrix; he = part of the haustorial encasement; pcw = plant cell wall; v = vacuole. **D,** Parts of a multilobed nucleus (n) and a plastid (p) with starch (s) and numerous plastoglobuli in a cell of the infected pepper leaf. See also Supplemental Figure 3 for more details on plastid ultrastructure; i = intercellular space; pcw = plant cell wall; v = vacuole.

ever, using RNA as template also presents challenges. For example, genes change their expression levels under different growing circumstances or during different pathogen developmental stages. Also, we showed that the *L. taurica* DNA isolated from infected leaves can be correctly measured using this standard curve and the relative quantification of *L. taurica* DNA accorded with their DI scores. Thus, using *L. taurica* DNA for quantification is reliable. One important note is that, when applying the

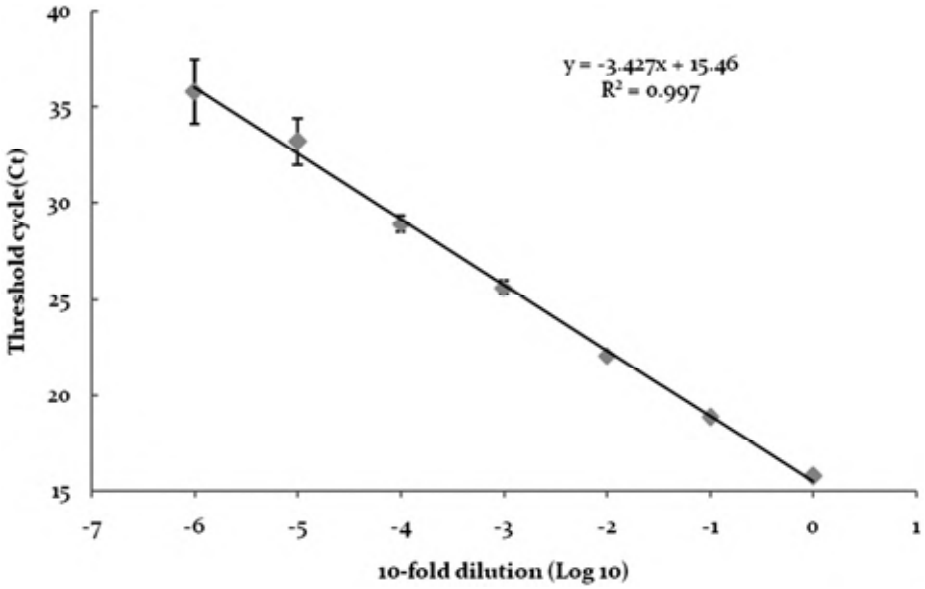

Fig. 7. Standard curve made by plotting threshold cycle (Ct) against a 10-time dilution series of genomic DNA, starting with 5,800 pg of *Leveillula taurica* DNA. The efficiency of the curve is 95.8%, with a correlation coefficient 0 to 9.978 and a slope of −3.4277. The experiment was repeated by using DNA isolated from an independent experiment.

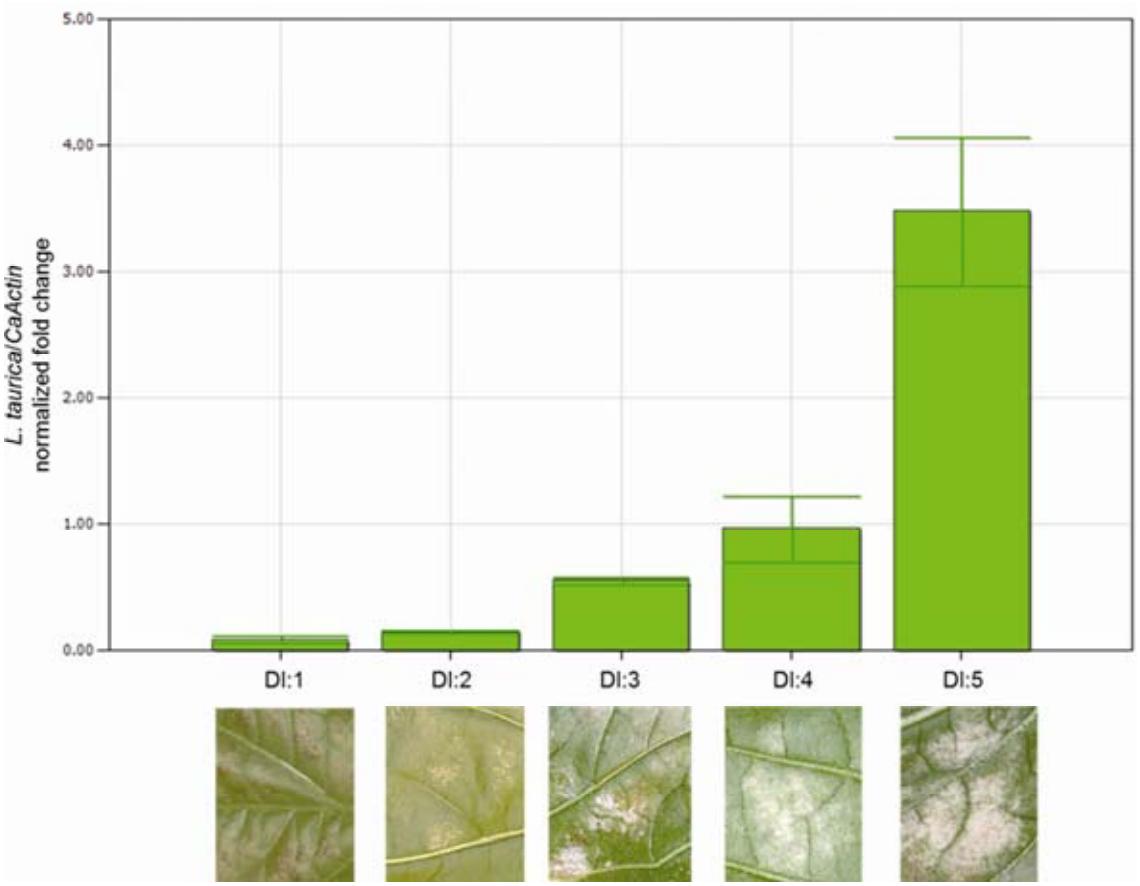

Fig. 8. Detection and quantification of *Leveillula taurica* DNA in pepper cultivars. Five cultivars were assigned with a different disease index (DI) and the mean DI score of three plants per cultivar is presented. To test the relative quantification methods, two infected leaves per plant were pooled for DNA isolation and two technical replications for quantitative reverse-transcription polymerase chain reaction (qRT-PCR) were used. Results were normalized by the ΔΔ cycle threshold method with *CaActin* as the reference gene. Error bars indicate the standard deviation. The experiment was repeated three times by taking different leaf samples of the same DI classes from the same plant. The Y-axis represents the fungal DNA amount relative to plant DNA in the infected leaves sampled and used for qRT-PCR.

detection method involving the absolute amount of *L. taurica* DNA in the host tissues, we used plant leaves of similar size for DNA isolation. If the plant tissue cannot be controlled for similar size or amount, the relative quantification method is more recommended for disease evaluation than using the *L. taurica* DNA standard curve.

The real-time PCR assay measures the fungal biomass and the DI scoring system represents the symptoms caused by fungal infection. Neither of these two systems is correlated with stages of fungal infection. According to the infection process shown by microscopic images in this study, the fungus has finished a complete cycle of infection when a plant is scored with a DI > 2. However, when a plant has a DI of 0 or 1 (generally regarded as a resistant plant), it is difficult to judge, without microscopic observation, which is the stage when the fungal growth is stopped. The newly developed real-time PCR assay makes it possible to produce a correlation curve between fungal biomass and each infection stage before sporulation. With such a curve, one may likely predict whether the fungal growth stops at penetration stage or intracellular growth stage. Today, several powdery mildew species have been sequenced and secreted effector proteins are being discovered. Generally, powdery mildew effectors are highly expressed in haustoria (31). Thus, there is a potential in the future to use cDNA for real-time PCR assay to monitor the expression level of haustorium-expressed effectors. In such a way, it is possible to predict when the fungal growth is stopped in a resistant plant.

In conclusion, the real-time PCR assays described in this study were shown to be quantitative, sensitive, and reproducible. Low amounts of *L. taurica* DNA could be quantified in the DNA sample of infected plants (Fig. 8). The relative quantification assay has the potential to be utilized as a convenient tool in breeding for resistance to powdery mildew disease. For studying the host–*L. taurica* interaction, the well-defined fungal infection process provides a basis for future study on mechanisms underlying resistance or susceptibility; for example, to monitor at which infection stage plant defense-related genes are up- or down-regulated. The potential of correlating the fungal infection stages with fungal biomass by real-time PCR offers a possibility to predict the failure stage of fungal growth.

ACKNOWLEDGMENTS

Z. Zheng and T. Nonomura contributed equally to this work. This work was supported by the Technology Top Institute-Green Genetics, the Netherlands (TTI-GG: 2CFD023RP), together with Monsanto Holland B.V., Nunhems Netherlands B.V., and Rijk Zwaan Zaadteelt en Zaadhandel B.V. The work done in Hungary was partly supported by a grant (LHNV2008) of the Hungarian National Development Agency (NFÜ) and a grant of the Hungarian Scientific Research Fund (OTKA K73565). In addition, the European Union and the European Social Fund have provided financial support to the project under the grant agreement number TÁMOP 4.2.1./B-09/1/KMR-2010-0003. We thank A.-M. Wolters for her critical reading of this manuscript.

LITERATURE CITED

1. Bai, Y., Huang, C.-C., van der Hulst, R., Meijer-Dekens, F., Bonnema, G., and Lindhout, P. 2003. QTLs for tomato powdery mildew resistance (*Oidium lycopersici*) in *Lycopersicon parviflorum* G1.1601 co-localize with two qualitative powdery mildew resistance genes. Mol. Plant-Microbe Interact. 16:169-176.
2. Bock, C. H., Parker, P. E., Cook, A. Z., and Gottwald, T. R. 2008. Visual rating and the use of image analysis for assessing different symptoms of citrus canker on grapefruit leaves. Plant Dis. 92:530-541.
3. Boyle, B., Hamelin, R. C., and Séguin, A. 2005. In vivo monitoring of obligate biotrophic pathogen growth by kinetic PCR. Appl. Environ. Microbiol. 71:1546-1552.
4. Braun, U., and Cook, R. T. A. 2012. Pages 1-707 in: Taxonomic Manual of the *Erysiphales* (Powdery Mildews). CBS-KNAW Fungal Biodiversity Centre, Utrecht, The Netherlands.
5. Clerk, G. C., and Ayesu-Offei, E. N. 1967. Conidia and conidial germination in *Leveillula taurica* (Lèv.) Arn. Ann. Bot. 31:749-755.
6. Daubèze, A. M., Hennart, J. W., and Palloix, A. 1995. Resistance to *Leveillula taurica* in pepper (*Capsicum annuum*) is oligogenically controlled and stable in Mediterranean regions. Plant Breed. 114:327-332.
7. de Souza, V. L., and Café-Filho, A. C. 2003. Resistance to *Leveillula taurica* in the genus *Capsicum*. Plant Pathol. 52:613-619.
8. Gáborjányi, R., Almási, A., Sárvári, É., Bóka, K., Lózsa, R., and Sági, Z. 2006. Ultrastructural changes of chloroplasts caused by tobamovirus infections in different pepper varieties. Cereal Res. Commun. 34:449-452.
9. Gachon, C., and Saindrenan, P. 2004. Real-time PCR monitoring of fungal development in *Arabidopsis thaliana* infected by *Alternaria brassicicola* and *Botrytis cinerea*. Plant Physiol. Biochem. 42:367-371.
10. Gardner, R. M., Tindall, G. W., Cline, S. M., and Brown, K. L. 1993. Ergosterol determination in activated sludge and its application as a biochemical marker for monitoring fungal biomass. J. Microbiol. Methods 17:49-60.
11. Harrison, J. G., Barker, H., Lowe, R., and Rees, E. A. 1990. Estimation of amounts of *Phytophthora infestans* mycelium in leaf tissue by enzyme-linked-immunosorbent-assay. Plant Pathol. 39:274-277.
12. Homma, Y., Arimoto, Y., Takahashi, H., Ishikawa, T., Matsuda, I., and Misato, T. 1980. Studies on pepper powdery mildew I. Conidial germination, hyphal elongation and hyphal penetration on pepper leaf. Ann. Phytopathol. Soc. Jpn. 46:140-149.
13. Khodaparast, S. A., Niinomi, S., and Takamatsu, S. 2007. Molecular and morphological characterization of *Leveillula* (Ascomycota: *Erysiphales*) on monocotyledonous plants. Mycol. Res. 111:673-679.
14. Khodaparast, S. A., Takamatsu, S., Harada, M., Abbasi, M., and Samadi, S. 2012. Additional rDNA ITS sequences and its phylogenetic consequences for the genus *Leveillula* with emphasis on conidium morphology. Mycol. Prog. 11:741-752.
15. Khodaparast, S. A., Takamatsu, S., and Hedjaroude, G.-A. 2001. Phylogenetic structure of the genus *Leveillula* (*Erysiphales: Erysiphaceae*) inferred from the nucleotide sequences of the rDNA ITS region with special reference to the *L. taurica* species complex. Mycol. Res. 105:909-918.
16. Kiss, L. 2012. Limits of nuclear ribosomal DNA internal transcribed spacer (ITS) sequences as species barcodes for Fungi. Proc. Natl. Acad. Sci. USA 109:E1811.
17. Kunoh, H., Kohno, M., Tashiro, S., and Ishizaki, H. 1979. Studies of the powdery-mildew fungus, *Leveillula taurica*, on green pepper. II. Light and electron microscopic observation of the infection process. Can. J. Bot. 57:2501-2508.
18. Laurans, F., and Pilate, G. 1999. Histological aspects of a hypersensitive response in poplar to *Melampsora larici-populina.* Phytopathology 89:233-238.
19. Lefebvre, V., Daubèze, A.-M., van der Voort, J. R., Peleman, J., Bardin, M., and Palloix, A. 2003. QTLs for resistance to powdery mildew in pepper under natural and artificial infections. Theor. Appl. Genet. 107:661-666.
20. Livak, K. J., and Schmittgen, T. D. 2001. Analysis of relative gene expression data using real-time quantitative PCR and the $2^{-\Delta\Delta CT}$ method. Methods 25:402-408.
21. McCartney, H. A., Foster, S. J., Fraaije, B. A., and Ward, E. 2003. Molecular diagnostics for fungal plant pathogens. Pest Manag. Sci. 59:129-142.
22. Micali, C. O., Neumann, U., Grunewald, D., Panstruga, R., and O'Connell, R. 2011. Biogenesis of a specialized plant-fungal interface during host cell internalization of *Golovinomyces orontii* haustoria. Cell. Microbiol. 13:210-226.
23. Newton, A. C., and Reglinski, T. 1993. An enzyme-linked-immunosorbent-assay for quantifying mildew biomass. Z. Pflanzenkrankh. Pflanzenschutz J. Plant Dis. Prot. 100:176-179.
24. Nonomura, T., Matsuda, Y., Xu, L., Kakutani, K., Takikawa, Y., and Toyoda, H. 2009. Collection of highly germinative pseudochain conidia of *Oidium neolycopersici* from conidiophores by electrostatic attraction. Mycol. Res. 113:364-372.
25. Pacovsky, R. S., and Bethlenfalvay, G. J. 1982. Measurement of the extraradical mycelium of a vesicular-arbuscular mycorrhizal fungus in soil by chitin determination. Plant Soil 68:143-147.
26. Sameshima, T., Kashimoto, K., Kida, K., Matsuda, Y., Nonomura, T., Kakutani, K., Nakata, K., Kusakari, S., and Toyoda, H. 2004. Cytological events in tomato leaves inoculated with conidia of *Blumeria graminis* f. sp. *hordei* and *Oidium neolycopersici* KTP-01. J. Gen. Plant Pathol. 70:7-10.
27. Šašek, V., Nováková, M., Jindřichová, B., Bóka, K., Valentová, O., and Burketová, L. 2012. Recognition of avirulence gene *AvrLm1* from hemibiotrophic ascomycete *Leptosphaeria maculans* triggers salicylic acid and ethylene signaling in *Brassica napus*. Mol. Plant-Microbe Interact. 25:1238-1250.

28. Schoch, C. L., Seifert, K. A., Huhndorf, S., Robert, V., Spouge, J. L., Levesque, C. A., Chen, W., and Consortium, F. B. 2012. Nuclear ribosomal internal transcribed spacer (ITS) region as a universal DNA barcode marker for fungi. Proc. Natl. Acad. Sci. USA 109:6241-6246.
29. Shifriss, C., Pilowsky, M., and Zacks, J. 1992. Resistance to *Leveillula taurica* mildew (=*Oidiopsis taurica*) in *Capsicum annuum*. Phytoparasitica 20:279-283.
30. Silvar, C., Merino, F., and Díaz, J. 2008. Differential activation of defense-related genes in susceptible and resistant pepper cultivars infected with *Phytophthora capsici.* J. Plant Physiol. 165:1120-1124.
31. Spanu, P. D., Abbott, J. C., Amselem, J., Burgis, T. A., Soanes, D. M., Stüber, K., Loren van Themaat, E. V., Brown, J. K. M., Butcher, S. A., Gurr, S. J., Lebrun, M.-H., Ridout, C. J., Schulze-Lefert, P., Talbot, N. J., Ahmadinejad, N., Ametz, C., Barton, G. R., Benjdia, M., Bidzinski, P., Bindschedler, L. V., Both, M., Brewer, M. T., Cadle-Davidson, L., Cadle-Davidson, M. M., Collemare, J., Cramer, R., Frenkel, O., Godfrey, D., Harriman, J., Hoede, C., King, B. C., Klages, S., Kleemann, J., Knoll, D., Koti, P. S., Kreplak, J., López-Ruiz, F. J., Lu, X., Maekawa, T., Mahanil, S., Micali, C., Milgroom, M. G., Montana, G., Noir, S., O'Connell, R. J., Oberhaensli, S., Parlange, F., Pedersen, C., Quesneville, H., Reinhardt, R., Rott, M., Sacristán, S., Schmidt, S. M., Schön, M., Skamnioti, P., Sommer, H., Stephens, A., Takahara, H., Thordal-Christensen, H., Vigouroux, M., Weßling, R., Wicker, T., and Panstruga, R. 2010. Genome expansion and gene loss in powdery mildew fungi reveal tradeoffs in extreme parasitism. Science 330:1543-1546.
32. Thomson, S. V., and Jones, W. B. 1981. An epiphytotic of *Leveillula taurica* on tomatoes in Utah. Plant Dis. 65:518-519.
33. Tisserant, B., Gianinazzi-Pearson, V., Gianinazzi, S., and Gollotte, A. 1993. In planta histochemical staining of fungal alkaline phosphatase activity for analysis of efficient arbuscular mycorrhizal infections. Mycol. Res. 97:245-250.
34. Viljanen-Rollinson, S. L. H., Gaunt, R. E., Frampton, C. M. A., Falloon, R. E., and McNeil, D. L. 1998. Components of quantitative resistance to powdery mildew (*Erysiphe pisi*) in pea (*Pisum sativum*). Plant Pathol. 47:137-147.
35. Vincelli, P., and Tisserat, N. 2008. Nucleic acid-based pathogen detection in applied plant pathology. Plant Dis. 92:660-669.
36. Voegele, R. T., and Schmid, A. 2011. RT real-time PCR-based quantification of *Uromyces fabae* in planta. FEMS Microbiol. Lett. 322:131-137.
37. Winton, L. M., Stone, J. K., Watrud, L. S., and Hansen, E. M. 2002. Simultaneous one-tube quantification of host and pathogen DNA with real-time polymerase chain reaction. Phytopathology 92:112-116.